VSP

Journal of Adhesion Science and Technology 24 (2010) 2693–2705

Journal of ADHESION SCIENCE and TECHNOLOGY
brill.nl/jast

Fabrication of Novel Superhydrophobic Surfaces and Water Droplet Bouncing Behavior — Part 1: Stable ZnO–PDMS Superhydrophobic Surface with Low Hysteresis Constructed Using ZnO Nanoparticles

Bin-Bin Wang [a], **Jiang-Tao Feng** [a], **Ya-Pu Zhao** [a,*] **and T. X. Yu** [b]

[a] State Key Laboratory of Nonlinear Mechanics, Institute of Mechanics, Chinese Academy of Sciences, Beijing 100190, China

[b] Department of Mechanical Engineering, Hong Kong University of Science and Technology, Clear Water Bay, Kowloon, Hong Kong SAR, China

Abstract

A superhydrophobic surface has many advantages in micro/nanomechanical applications, such as low adhesion, low friction and high restitution coefficient, etc. In this paper, we introduce a novel and simple route to fabricate superhydrophobic surfaces using ZnO nanocrystals. First, tetrapod-like ZnO nanocrystals were prepared *via* a one-step, direct chemical vapor deposition (CVD) approach. The nanostructured ZnO material was characterized by scanning electron microscope (SEM) and X-ray diffraction (XRD) and the surface functionalized by aminopropyltriethoxysilane (APS) was found to be hydrophobic. Then the superhydrophobic surface was constructed by depositing uniformly ZnO hydrophobic nanoparticles (HNPs) on the Poly(dimethylsiloxane) (PDMS) film substrate. Water wettability study revealed a contact angle of $155.4 \pm 2°$ for the superhydrophobic surface while about 110° for pure smooth PDMS films. The hysteresis was quite low, only $3.1 \pm 0.3°$. Microscopic observations showed that the surface was covered by micro- and nano-scale ZnO particles. Compared to other approaches, this method is rather convenient and can be used to obtain a large area superhydrophobic surface. The high contact angle and low hysteresis could be attributed to the micro/nano structures of ZnO material; besides, the superhydrophobic property of the as-constructed ZnO–PDMS surface could be maintained for at least 6 months.

Keywords

Superhydrophobic surface, contact angle hysteresis, ZnO, PDMS, surface modifications

Notations

R radius of contact area

δ average distance between liquid and solid molecules

* To whom correspondence should be addressed. Fax: +86-10-6256-1284; e-mail: yzhao@imech.ac.cn

DOI:10.1163/016942410X508244

ε restitution coefficient

θ contact angle

γ surface/interface tension

σ line tension

Subscripts

L liquid

S solid

s stable

V vapor

List of Abbreviations

APS	aminopropyltriethoxysilane
CA	contact angle
CAH	contact angle hysteresis
CD	constant diameter
CVD	chemical vapor deposition
HNPs	hydrophobic nanoparticles
MEMS	microelectromechanical systems
NEMS	nanoelectromechanical systems
PDMS	poly(dimethylsiloxane)
SCCM	standard cubic centimeter per minute
SEM	scanning electron microscope
XRD	X-ray diffraction

1. Introduction

Numerous micro/nanotribological and micro/nanomechanical applications, such as in micro/nanoelectromechanical systems (MEMS/NEMS) require surfaces with low adhesion and friction [1]. As the size of these devices decreases, the surface forces tend to dominate over the volume forces, and adhesion and 'stiction' constitute a challenging problem for proper operation of these devices. This makes the development of nonadhesive surfaces crucial for many of these applications. With this background, the so called 'superhydrophobic' or 'ultrahydrophobic' surfaces

and their corresponding properties have attracted the attention of many researchers all over the world. Superhydrophobic surfaces have been applied in MEMS field especially in electrowetting research. Kakade *et al.* [2] fabricated superhydrophobic multiwalled carbon nanotube bucky paper showing fascinating electrowetting behavior. The droplet behavior can be reversibly switched between superhydrophobic Cassie–Baxter state to hydrophilic Wenzel state by the application of an electric field, especially below a threshold value. Bahadur and Garimella analyzed the influence of applied voltage in determining and altering the state of a static droplet resting on a superhydrophobic surface [3]. In general, surfaces with a static contact angle (CA) higher than 150° are defined as superhydrophobic surfaces [4–8]. Large CA or limited contact area reduces the adhesion or friction between liquid droplets and solid surfaces. Thus the CA is a measure of adhesion between water and solid surface. However, in some cases, contact angle hysteresis (CAH) is more important than maximum CA since CAH is directly related to driving force for a liquid drop [9]. For example, liquid flow requires low solid–liquid friction. That is, in addition to high contact angle, a superhydrophobic surface should also have very low water CAH. The condition of CAH $< 10°$ may be a good suggestion for claiming superhydrophobicity [6, 10].

A third wetting characteristic for a superhydrophobic surface, in addition to a high CA and low CAH, has been proposed by some researchers [11, 12], i.e., the ability of the surface to bounce off droplets. It has been shown that this ability is related to energy barriers associated with the transition between the Cassie [13] and Wenzel [14] wetting states. From energy consideration, the Cassie–Baxter state is often metastable. In practice, this means that the drop will remain in a Cassie–Baxter state only if it is subjected to small external perturbations. However, as for the definition of a superhydrophobic surface, there is no consensus whether restitution coefficient ε should be considered. Furthermore, ε first increases with increasing velocity, and then stays at a constant value (stable restitution coefficient ε_s) almost independent of the velocity. Thus, $\varepsilon_s > 0.8$ may be a good suggestion from the viewpoint of rebound of droplets from a superhydrophobic surface.

However, the static CA of a superhydrophobic surface is higher than 150° generally, but the impact of hysteresis is still controversial. And the ability of a surface to bounce off droplets has received relatively less attention. In the current decade, there has been an explosion of publications describing how surface topography can be used to control wettability. A large number of ways to produce superhydrophobic surfaces have been investigated using many and different materials [15]. Thus, zinc oxide (ZnO), an excellent candidate for the fabrication of electronic and optoelectronic nanodevices, was also studied. Many efforts have been focused on the fabrication of ZnO based superhydrophobic films. Badre *et al.* successfully prepared ZnO films with well-controlled morphologies by electrochemical deposition [16]. In their work, a seed layer of nanocrystallites of ZnO was prepared from which ZnO nanowires were grown. Then, a treatment with alkylsilane yielded superhydrophobic surfaces. Badre *et al.* [17] also prepared highly water-

repellent surfaces from arrays of ZnO nanowires by treatment with stearic acid. They attributed the superhydrophobic properties to a micro-nano binary structure combined with a low surface free energy. Berger *et al.* [18] fabricated ZnO crystals arrays by employing hydrothermal approach and the hydrophobicity of the films could be regulated by regulating zinc ion precursor concentration. The CA on these surfaces increased from 110° to 156° with decreasing concentration of zinc ion precursor, demonstrating controllable wetting behavior. Liu *et al.* [19] fabricated ZnO films by Au-catalyzed chemical vapor deposition (CVD) method. The surface of as-synthesized film exhibited hierarchical structure with sub-microstructures with CA about 164.3°, and UV illumination could switch the surface from hydrophobic to hydrophilic. Another way to synthesize a ZnO film is direct oxidation of Zn substrate. Using this method, Hou *et al.* [20] prepared the ZnO film on zinc layer successfully, and the surface was hydrophobically functionalized with n-octadecyl thiol. The modified ZnO film exhibited superhydrophobicity and the water contact angle was $153 \pm 2°$.

The methods used above have their own drawbacks. The hydrothermal method and electrochemical deposition are relatively complex and difficult to apply for mass production. As for the CVD method [19] mentioned above, a catalyst is needed for the growth of ZnO film which means the catalyst layer should be deposited on the substrate in advance. As for direct oxidation method, a Zn seed layer is needed to produce a superhydrophobic surface. Thus the area of as-fabricated surface is limited to the area of seed layer. In this paper, we propose a simple method to fabricate superhydrophobic surfaces by ZnO nanomaterials. The synthesis of ZnO nanomaterials was carried using CVD method. Also in this study, we combined CVD method and surface modification process to fabricate ZnO-based superhydrophobic surfaces, which opens a new potential application for ZnO nanomaterials synthesized by CVD method. Compared to other ways to construct ZnO hydrophobic surfaces, our method is convenient and can be used to fabricate large area surfaces. The contact angle is $155.4 \pm 2°$, and the hysteresis of the superhydrophobic surface is quite low ($3.1 \pm 0.3°$), which means that the surface has self-cleaning property. Besides, the superhydrophobic properties are stable and durable for at least 6 months.

2. Experimental

2.1. Preparation of ZnO Powder

The nanostructured ZnO material was synthesized *via* a simple catalyst-free CVD method [21–23]. The main parameters of CVD method to synthesize ZnO nanomaterials are temperature and gas flow rate. Temperature should be higher than the melting point of Zn (419.6°C) and thus Zn would be in liquid state. So Zn vapor could react with O_2 to form nanostructured ZnO. However, the temperature cannot be too high, otherwise the reaction rate would be too fast and regular ZnO nanostructures would not be found. Gas flow rate is another parameter, as a low O_2 partial

pressure could also limit the react rate. In the experiments mentioned in this paper, 640°C and 20 SCCM O_2 flow were found to be proper conditions to synthesize regular ZnO nanotetrapods. The process used was as follows. First, about 2.0 g Zn powder (99.999%) was evenly dispersed on the bottom of an alumina boat which was placed in the middle of a quartz tube. The tube was placed horizontally in a high-temperature tubular furnace. Then, a silicon substrate was placed face-down on the boat. The materials were heated at a moderate rate of about 30°C min^{-1}. When the desired temperature (640°C) was reached, Ar at a flow rate of about 300 SCCM (SCCM denotes standard cubic centimeter per minute at STP) and O_2 at about 20 SCCM were introduced into the system and maintained for 20 min. Finally, the flows of Ar and O_2 were shut down. White ZnO material was collected on the surface of the substrate after the furnace was cooled naturally down to room temperature.

2.2. Surface Modification of ZnO Powder and Fabrication of Superhydrophobic Surface

The micro/nano scale ZnO powder synthesized by CVD method usually agglomerated, thus the material needed to be treated to obtain dispersed particles. First, the as-synthesized ZnO powder was dispersed in ethyl alcohol which was contained in a beaker. Then the suspension was treated with supersonic waves for about 20 min, and the upper suspension was collected in another beaker. This process was repeated four times in order to avoid large particles. To prevent the strong aggregation effect of ZnO nano-particles, aminopropyltriethoxysilane (APS) was added to the suspension [22, 23]. The mass ratio of ZnO, alcohol and APS was 1:100:0.1. Then the suspension was dried in a drying oven and the as-treated ZnO material was ground into a powder. In this process, the APS was used to weaken the agglomeration tendency as well as to enhance the hydrophobicity of the ZnO particles.

The superhydrophobic surface was fabricated on a poly (dimethylsiloxane) (PDMS) film. First, the silicone elastomer base and curing agent were mixed uniformly and the mass ratio was 10:1. PDMS (SYLGARD) and curing agent were procured from Dow Corning Corporation, Midland, Michigan, USA. The mixture of PDMS and curing agent was stirred adequately. The modified ZnO particles were dispersed on the half-dry PDMS film evenly, and then the film was placed in the oven again until solidification was completed. The superhydrophobic ZnO–PDMS surface formed after rinsing the film with deionized water to remove loose ZnO particles.

2.3. Characterization

The morphologies of ZnO powder samples and the ZnO–PDMS surface were characterized with a scanning electron microscope (SEM) (FESEM FEI SIRION) and an optical microscope DZ3 (Union, Japan), respectively. The crystalline structure of the ZnO material obtained was examined by X-ray powder diffraction (XRD) on an X-ray diffractometer D/MAX-2500 (Rigaku, Japan). Furthermore, X-ray photo-

electron spectroscopy (XPS) was employed to investigate the surface properties of ZnO particles. Water contact angle characterization of ZnO samples was carried out using an OCA 20 (Dataphysics, Germany) contact angle analyzer.

3. Results and Discussion

3.1. Structure and Morphology Characterization

The SEM micrographs of as-synthesized ZnO material are shown in Fig. 1(f) and 1(g). The ZnO material is found to be tetrapod-like, and the legs are 4–10 μm long. The diameter of each leg is about 200–500 nm. The micrograph with larger magnification in Fig. 1(g) shows that the ZnO particles have submicrometer structures.

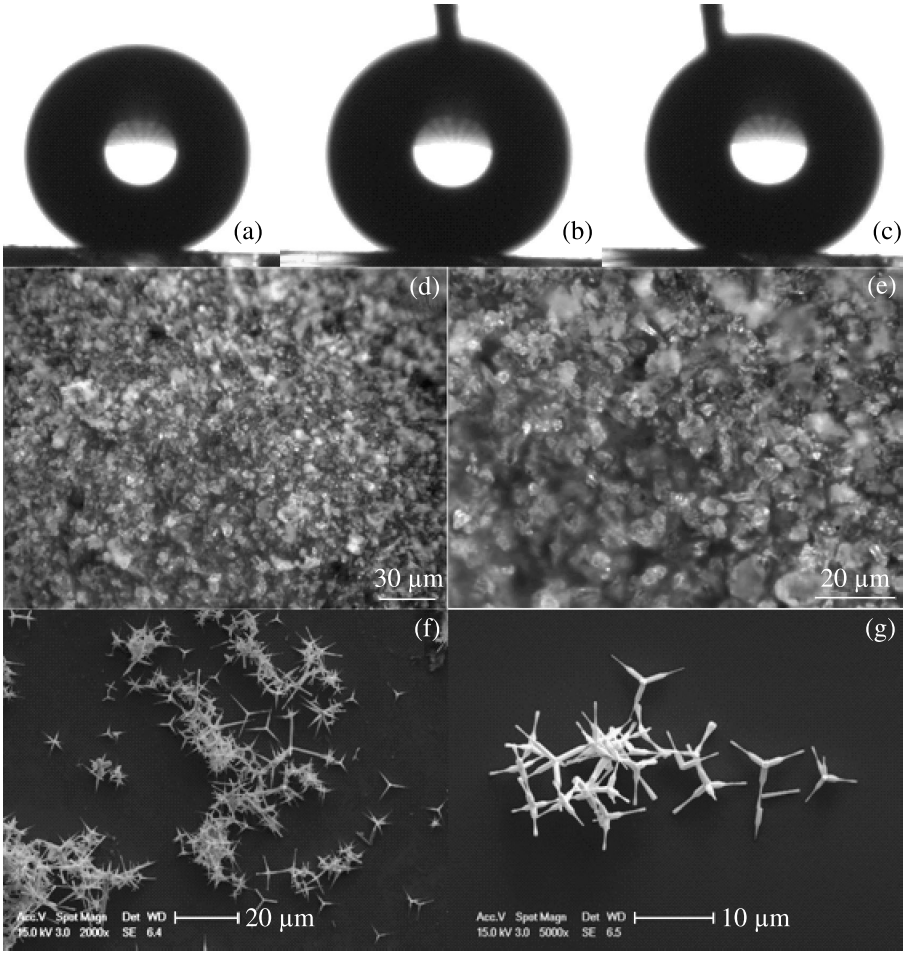

Figure 1. (a)–(c) ZnO–PDMS surface: (a) static contact angle, (b) advancing angle, and (c) receding angle. (d)–(e) Surface morphology of ZnO–PDMS surface constructed by coating PDMS film with ZnO particles. (f)–(g) SEM micrographs of as-synthesized ZnO particles with tetrapod shape.

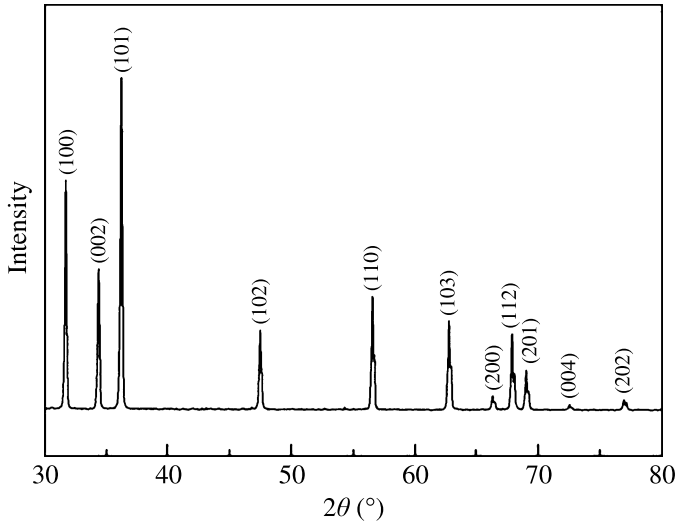

Figure 2. X-ray diffraction pattern of ZnO.

The crystal structure of the ZnO tetrapods was examined with XRD as shown in Fig. 2. The sharp and strong peaks suggested that the products were highly crystalline. All these XRD peaks could be indexed as the hexagonal wurtzite ZnO, with the lattice constants $a = 3.253$ Å and $c = 5.209$ Å. No peaks of zinc or other impurities were found in the pattern, which showed that the tetrapods were rather pure ZnO wurtzite.

The pictures of the superhydrophobic surface taken by an optical microscope are shown in Fig. 1(d) and 1(e). It was found that the tetrapod-like structure of ZnO particles was destroyed during surface modification process, and only a few particles remained as tetrapods in shape. The distribution and outline of the particles are random and irregular, and the diameters of particles range from 3.8 to 10.3 μm. Furthermore, the distance between the particles was also about several micrometers, thus the roughness is considered to be of the same magnitude.

3.2. Floating Test and XPS Examination

In order to study the surface characteristics, non-modified and APS-modified ZnO particles were analyzed by floating test measurements [20]. The floating test was used to measure the ratio of the floated product to the overall weight of the sample after it was mixed in water and stirred vigorously. The ratio above was called the active ratio. Without the addition of silane, the ZnO particles obtained were hydrophilic, and the active ratio was 0.0%. When the ZnO particles were treated with APS, the active ratios of all the samples were above 90.5%. The floating test demonstrates that the hydrophobic organic (APS) molecules had been bonded to the surfaces of the obtained modified ZnO particles, as the hydrophobic property of modified ZnO particles remained even after the particles were washed with hot water and alcohol. Figure 3(a)–(c) shows XPS spectra for the as-treated ZnO mate-

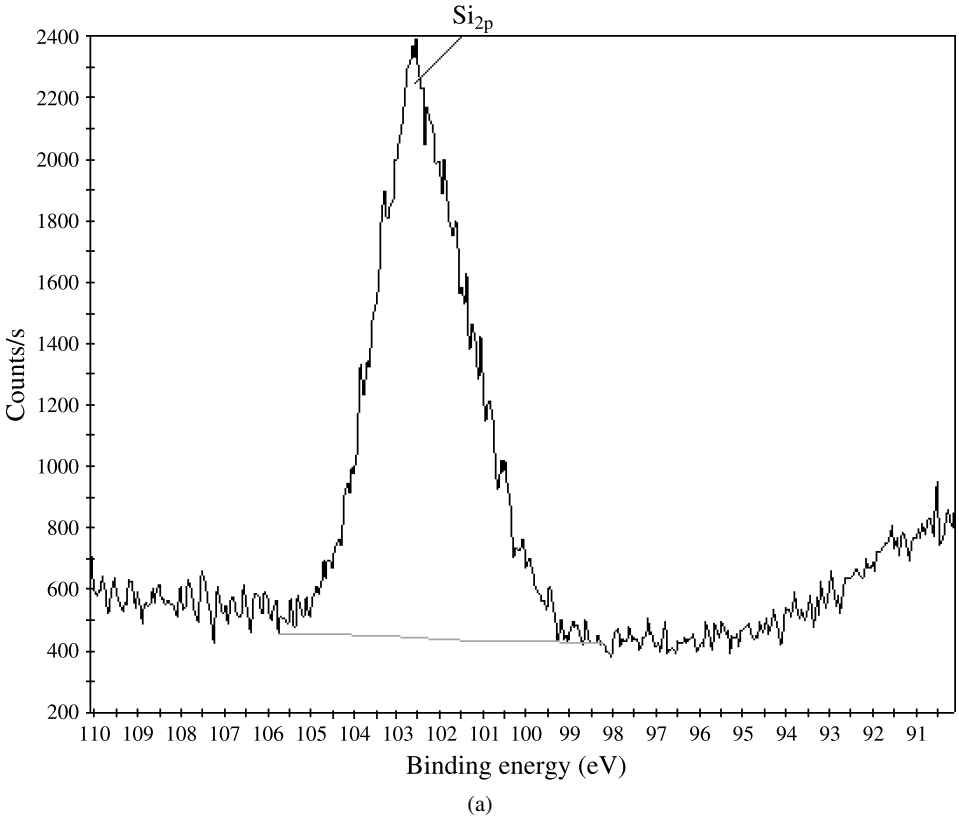

Figure 3. XPS spectra for the ZnO material treated with APS: (a) Si scan. (b) N scan. (c) C scan.

rial. The results indicate that APS is coated on the surface of ZnO particles. Hence, the APS could reduce aggregation and enhance the hydrophobicity of the particles effectively.

3.3. Wettability Study of the Superhydrophobic Surface

The hydrophobic property of the fabricated surface was investigated by contact angle measurements with a precision of $\pm 0.1°$, and the smooth PDMS surface was also studied for comparison. Advancing and receding contact angles were measured by adding to and withdrawing liquid from the droplet, respectively. CAs were recorded after they became stable and were checked on several films. The volume of water droplets used for CA measurements was 3.65 μl, and the diameter was about 0.98 mm. Some typical results on ZnO–PDMS surface are shown in Fig. 1(a)–(c). It was found that the contact angle was only 114.5° for smooth PDMS surface, while the contact angle of the superhydrophobic surface was about $155.4 \pm 2°$. The advancing and receding angles of PDMS surface were 119.6° and 102.2°, respectively. The CAH of the superhydrophobic surface is very low ($3.1 \pm 0.3°$), and the droplet could hardly stay on the surface during the experiment. Compared to smooth

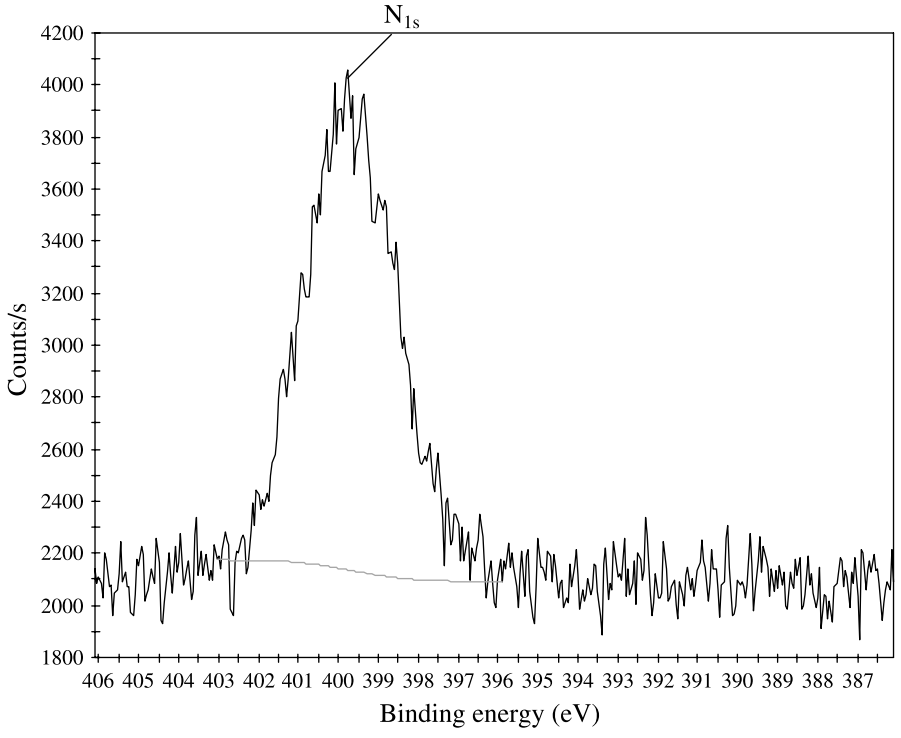

(b)

Figure 3. (Continued).

PDMS surface, the superhydrophobic surface constructed by ZnO nanocrystals has much larger CA and smaller CAH. For comparison, the wettability of flat Si substrate modified by APS was studied and CA was found to be 11.9°, which showed that the APS formed a hydrophilic coating. Besides, the superhydrophobicity of ZnO–PDMS surface could be maintained for at least 6 months without any change. Furthermore, we have tested several kinds of silanes including methyltriethoxysilane and ethyltriethoxysilane hoping to find the differences or trends between the three silanes. However, the differences were found on a flat substrate but no significant differences were observed on fabricated superhydrophobic surfaces using the same technique (less than 5°). So only the APS experiments were shown in this paper.

3.4. Dependence of Contact Angle on Droplet Diameter

The static CAs of the droplets with different sizes were measured experimentally and the size dependence of contact angle was observed in our solid–liquid system. As shown in Fig. 4, the CA decreases from 155.9° to 134.2° while the size of droplet decreases due to evaporation. The diameters for the droplet are 1.72 mm, 1.55 mm, 1.42 mm, 1.30 mm, 1.22 mm, 1.09 mm, 0.97 mm, 0.82 mm, 0.66 mm and 0.53 mm, respectively, and the corresponding contact angles are

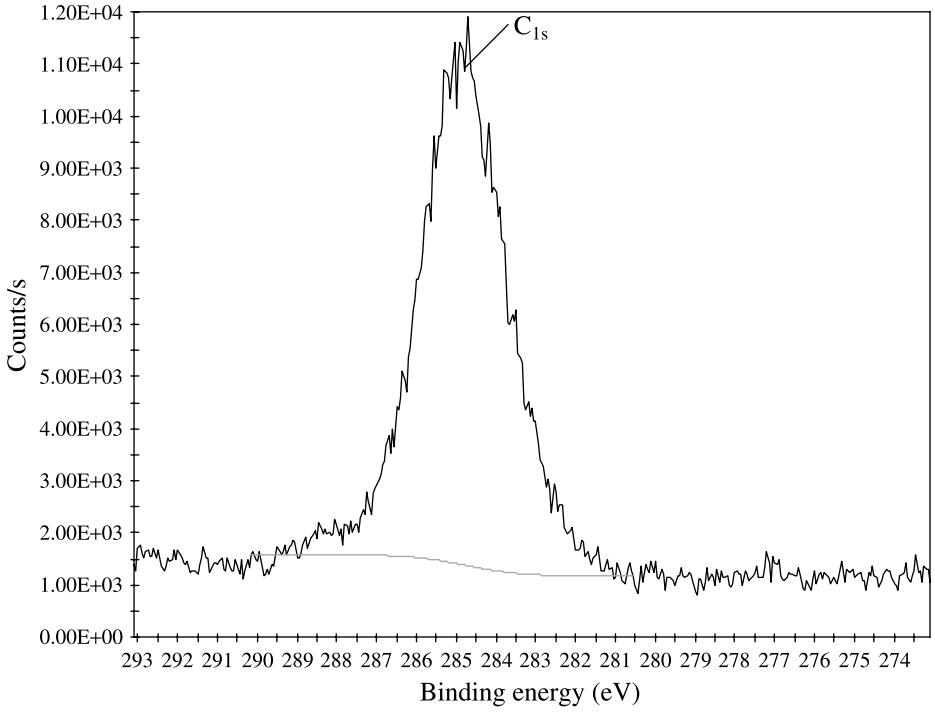

(c)

Figure 3. (Continued).

155.9°, 151.6°, 150.4°, 150.6°, 149.9°, 147.3°, 145.2°, 142.6°, 136.2° and 134.2°. The contact angle varies with the drop size from a few degrees up to 8.6°. This phenomenon has been studied by some researchers, and it was found that droplet follows the evaporation model normally ascribed to hydrophobic surfaces [24]. The size dependence effect could be explained in terms of the so-called line tension, or the tension at the three-phase contact line [25, 26]. The line tension σ, in analogy to surface tension, is defined as the specific free energy of the three-phase contact line or, mechanically, as a force operating at the three-phase line.

Taking line tension into account, the Young's equation can be modified as:

$$\gamma_{LV}\cos\theta = \gamma_{SV} - \gamma_{SL} - \frac{\sigma}{R}, \tag{1}$$

where R denotes the radius of contact area and θ denotes the contact angle.

From equation (1), we learn that the contact angle should increase with increasing drop diameter when the line tension σ is negative, and decrease when σ is positive. For the calculation of line tension, Marmur gave an approximate expression [27]:

$$\sigma \approx 4\delta\sqrt{\gamma_{SV}\gamma_{LV}}\cot\theta, \tag{2}$$

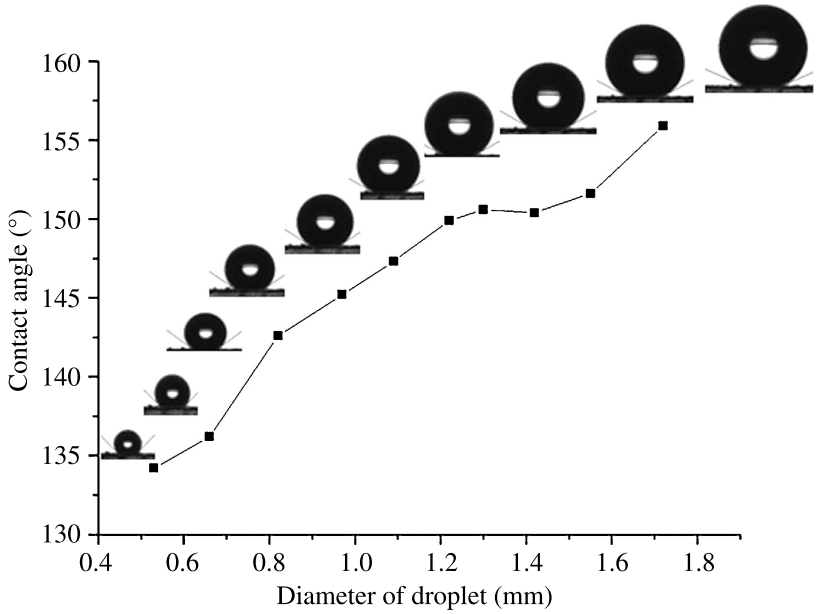

Figure 4. Contact angles of droplets with different diameters: (from right to left) the contact angles are 155.9°, 151.6°, 150.4°, 150.6°, 149.9°, 147.3°, 145.2°, 142.6°, 136.2° and 134.2°, respectively, and the diameters of droplets are 1.72 mm, 1.55 mm, 1.42 mm, 1.30 mm, 1.22 mm, 1.09 mm, 0.97 mm, 0.82 mm, 0.66 mm and 0.53 mm, respectively.

where δ denotes the average distance between liquid and solid molecules. Thus the line tension is negative for an obtuse CA, while σ is positive for an acute CA. As the CA was 134.2°–155.9°, so the line tension was negative in our experiment. Thus the CA should be an increasing function of droplet size, which is consistent with our experimental results.

3.5. Mechanism of Superhydrophobicity

The superhydrophobic properties of the surface are demonstrated by the CAs as shown in Fig. 1(a)–(c). Especially, the hysteresis is quite low, which means that the droplet could move on the surface very easily and the surface is self-cleaning. We attribute the superhydrophobic property to the micro/nano structure of the ZnO particles in the coating. As shown in Fig. 1(f) and 1(g), the as-synthesized ZnO material has micro/submicro structure. And Fig. 1(d) and 1(e) shows that the microparticles are about 1–10 μm in length, thus the roughness of the surface is considered to be of the same magnitude. The micro/nano structures lead to the porous structure of the coating and there is plenty of trapped air in the ZnO coating when the liquid droplet is placed on the surface. In such situation, the hydrophobic behavior relies on Cassie's law. Compared with Wenzel state, a superhydrophobic surface with Cassie state usually has larger contact angles and lower hysteresis. As for the superhydrophobic surface discussed here, the CA and CAH are $155.4 \pm 2°$ and

$3.1 \pm 0.3°$, respectively, which indicates that both adhesion and friction are relatively low. These two properties explain the fact that the droplet could hardly stay on the surface during the experiments.

Furthermore, APS was used to enhance the hydrophobicity and reduce aggregation of ZnO particles. APS has a flexible C4 hydrocarbon chain with one amino group that stretches out in a long zig-zag fashion to form a dense self-assembled layer of packed chains on ZnO as a result of the strong chelating bonds between triethoxy headgroups and Zn atoms on the surface. It is assumed that the layer of packed chains enhanced the hydrophobicity of ZnO particles. However, ASP by itself forms a 'hydrophilic' coating. As mentioned before, there were many trapped air bubbles between the liquid droplet and ZnO particles when the droplet was placed on the surface. Thus, the wettability of ZnO particles has less effect on the apparent CA compared to the porous structure. In a word, both the porous structure and the silane coating lead to the superhydrophobicity of the surface: CA of ZnO surface consisting of micro/nano particles is about $155.4 \pm 2°$ and the CAH is about $3.1 \pm 0.3°$.

However, from energy consideration, the Cassie state is usually metastable and there is energy barrier between Cassie state and Wenzel state. The transition between these two states could occur when fluctuation was introduced in the system. Another parameter, i.e., the energy barrier is associated with the ability of droplet to bounce off the surface [28], has been proposed as the third property of a superhydrophobic surface by some researchers [12]. The impact experiment between droplet and ZnO–PDMS surface and the influence of CAH on droplet dynamic behavior will be discussed separately.

4. Conclusions

A superhydrophobic ZnO–PDMS surface has been fabricated by depositing modified nanostructured ZnO material on the PDMS surface, which is quite convenient compared to other methods. In the experiments, silane was used to avoid the aggregation as well as to enhance the hydrophobicity of ZnO particles. The porous structure of the ZnO layer leads to its superhydrophobicity. Wettability study showed that the CA and CAH were $155.4 \pm 2°$ and $3.1 \pm 0.3°$, respectively. Besides, the superhydrophobicity could be maintained for at least six months without any change. The dependence of contact angle on droplet size was found on as-fabricated superhydrophobic surface, and showed that the static contact angle increased with increasing droplet size. The line tension theory gives a good explanation for this phenomenon. As both ZnO and PDMS have good biocompatibility, the ZnO–PDMS superhydrophobic surface is an interesting subject for further exploration and for possible applications in advanced semiconductor biological devices.

Acknowledgements

This work was jointly supported by the National High-tech R&D Program of China (863 Program, Grant No. 2007AA021803), National Basic Research Program of China (973 Program, Grant No. 2007CB310500), and National Natural Science Foundation of China (NSFC, Grant Nos 10772180, 60936001 and 10721202).

References

1. Y. P. Zhao, L. S. Wang and T. X. Yu, *J. Adhesion Sci. Technol.* **17**, 519 (2003).
2. B. Kakade, R. Mehta, A. Durge, S. Kulkarni and V. Pillai, *Nano Lett.* **8**, 2693 (2008).
3. V. Bahadur and S. V. Garimella, *Langmuir* **23**, 4918 (2007).
4. L. Gao and T. J. McCarthy, *Langmuir* **23**, 3762 (2007).
5. S. L. Ren, S. R. Yang, Y. P. Zhao, T. X. Yu and X. D. Xiao, *Surface Sci.* **546**, 64 (2003).
6. S. L. Ren, S. R. Yang and Y. P. Zhao, *Langmuir* **20**, 3061 (2004).
7. A. Lafuma and D. Quere, *Nature Mater.* **2**, 457 (2003).
8. J. Genzer and K. Efimenko, *Biofouling* **22**, 339 (2006).
9. J. T. Feng, F. C. Wang and Y. P. Zhao, *Biomicrofluidics* **3**, 022406 (2009).
10. B. Balu, V. Breedveld and D. W. Hess, *Langmuir* **24**, 4785 (2008).
11. S. Wang and L. Jiang, *Adv. Mater.* **19**, 3423 (2007).
12. M. Nosonovsky and B. Bhushan, *J. Phys.: Condens. Matter* **20**, 395005 (2008).
13. R. N. Wenzel, *Ind. Eng. Chem.* **28**, 988 (1936).
14. A. B. D. Cassie, *Trans. Faraday Soc.* **44**, 11 (1948).
15. A. Carré and K. L. Mittal (Eds), *Superhydrophobic Surfaces*. VSP/Brill, Leiden (2009).
16. C. Badre, T. Pauporte, M. Turmine, P. Dubot and D. Lincot, *Physica E* **40**, 7 (2008).
17. C. Badre, T. Pauporte, M. Turmine and D. Lincot, *Superlattice Microstructures* **42**, 99 (2007).
18. J. Berger, B. Englert, L. B. Zhu and C. P. Wong, in: *Proc. IEEE International Symposium and Exhibition on Advanced Packaging Materials and Processes*, Atlanta, GA, p. 93 (2006).
19. H. Liu, L. Feng, J. Zhai, L. Jiang and D. B. Zhu, *Langmuir* **22**, 5659 (2006).
20. X. M. Hou, F. Zhou, B. Yu and W. M. Liu, *Mater. Sci. Eng. A* **452**, 732 (2007).
21. F. Q. He and Y. P. Zhao, *Appl. Phys. Lett.* **88**, 193113 (2006).
22. F. Q. He and Y. P. Zhao, *J. Phys. D: Appl. Phys.* **39**, 2105 (2006).
23. B. B. Wang, J. J. Xie, Q. Z. Yuan and Y. P. Zhao, *J. Phys. D: Appl. Phys.* **41**, 102005 (2008).
24. S. A. Kulinich and M. Farzaneh, *Appl. Surface Sci.* **255**, 4056 (2009).
25. D. Q. Li, *Colloids Surfaces A* **116**, 1 (1996).
26. R. Tadmor, *Surface Sci.* **602**, L108 (2008).
27. A. Marmur, *J. Colloid. Interface Sci.* **186**, 462 (1997).
28. P. Brunet, F. Lapierre, V. Thomy, Y. Coffinier and R. Boukherroub, *Langmuir* **24**, 11203 (2008).